

# The sodium-calcium exchanger is a mechanosensitive transporter

John P. Reeves, Maha Abdellatif and Madalina Condrescu

Department of Pharmacology & Physiology, University of Medicine and Dentistry of New Jersey, Graduate School of Biomedical Sciences, 185 South Orange Avenue, Newark, NJ 07101-1709, USA

This report describes the influence of fluid flow and osmotically induced volume changes on  $\text{Na}^+$ – $\text{Ca}^{2+}$  exchange (NCX) activity in transfected CHO cells. Exchange activity was measured as  $\text{Na}^+$ -dependent  $\text{Ca}^{2+}$  or  $\text{Ba}^{2+}$  fluxes using the fluorescent probe fura-2. When exchange activity was initiated by superfusing  $\text{Ba}^{2+}$ -containing solutions over the cells for a 20 s interval, a high rate of  $\text{Ba}^{2+}$  uptake was observed while the solution was being applied but the rate of  $\text{Ba}^{2+}$  uptake declined > 10-fold when the solution flow ceased.  $\text{Ba}^{2+}$  efflux in exchange for extracellular  $\text{Na}^+$  or  $\text{Ca}^{2+}$  ( $\text{Ba}^{2+}$ – $\text{Ca}^{2+}$  exchange) was similarly biphasic. During NCX-mediated  $\text{Ca}^{2+}$  uptake, a rapid increase in cytosolic  $[\text{Ca}^{2+}]_i$  to a peak value occurred, followed by a decline in  $[\text{Ca}^{2+}]_i$  to a lower steady-state value after solution flow ceased. When NCX activity was initiated by an alternate procedure that minimized the duration of solution flow, the rapid phase of  $\text{Ba}^{2+}$  influx was greatly reduced in magnitude and  $\text{Ca}^{2+}$  uptake became nearly monophasic. Solution superfusion did not produce any obvious changes in cell shape or volume. NCX-mediated  $\text{Ba}^{2+}$  and  $\text{Ca}^{2+}$  influx were also sensitive to osmotically induced changes in cell volume. NCX activity was stimulated in hypotonic media and inhibited in hypertonic media; the osmotically induced changes in activity occurred within seconds and were rapidly reversible. We conclude that NCX activity is modulated by both solution flow and osmotically induced volume changes.

(Resubmitted 17 January 2008; accepted after revision 25 January 2008; first published online 31 January 2008)

**Corresponding author** J. P. Reeves: Department of Pharmacology & Physiology, University of Medicine and Dentistry of New Jersey, Graduate School of Biomedical Sciences, 185 South Orange Avenue, Newark, NJ 07101-1709, USA. Email: reeves@umdnj.edu

Many naturally occurring ion channels, as well as some artificial ones like gramicidin, are mechanosensitive, that is, they increase or decrease their activity in response to mechanical or osmotic stimuli (reviewed in Hamill & Martinac, 2001). Mechanosensitivity may be a common property of membrane proteins exhibiting multiple conformational states because some conformational transitions will inherently be sensitive to changes in membrane tension (Gu *et al.* 2001). This can be explained by the concept of 'hydrophobic mismatch' in which the hydrophobic portions of protein transmembrane segments in some conformations do not precisely match the hydrophobic dimensions of the lipid bilayer, leading to bending at the bilayer–protein interface to minimize the exposure of hydrophobic surfaces to the aqueous medium (Perozo *et al.* 2002; Hwang *et al.* 2003).

Channels may also be sensitive to shear forces generated during fluid flow. This is particularly important in endo-

thelial cells (Gautam *et al.* 2006), and in the cortical collecting ducts of the kidney (Satlin *et al.* 2006). The TRPM7 channel, which is stimulated by stretch and osmotic shock (Numata *et al.* 2007), also increases activity in response to laminar fluid flow (Oancea *et al.* 2006; Numata *et al.* 2007). Recent reports have described flow-dependent stimulation of L-type  $\text{Ca}^{2+}$  channel activity in transfected cells (Peng *et al.* 2005) and vascular myocytes (Park *et al.* 2007), and flow-dependent stimulation of electrical activity in cardiac myocytes (Kong *et al.* 2005; Lorenzen-Schmidt *et al.* 2006).

Some carrier-mediated transporters are mechanosensitive and function in the regulatory responses to osmotically induced changes in cell volume. For example, both the ubiquitous isoform of the  $\text{Na}^+$ – $\text{H}^+$  exchanger (NHE1) and the  $\text{Na}^+$ – $\text{K}^+$ – $2\text{Cl}^-$  cotransporter (NKCC1) increase their activities in response to a hyperosmotic stimulus, acting to increase the concentration of cytosolic osmolytes as part of the RVI (regulatory volume increase) response (reviewed in Pedersen *et al.* 2006). Other transporters, such as the taurine transporter, increase their

---

This paper has online supplemental material.

activity in response to a hypotonic stimulus, thereby promoting solute loss from the cytosol as part of the RVD (regulatory volume decrease) response (Lambert, 2004). The renal isoform of the  $\text{Na}^+-\text{H}^+$  exchanger (NHE3) responds in the opposite manner to NHE1, becoming inhibited in response to hyperosmolarity (Alexander & Grinstein, 2006). The  $\text{Na}^+, \text{K}^+$ -ATPase is also mechanosensitive, increasing its activity in response to a hypotonic stimulus and vice versa for a hypertonic stimulus (Venosa, 1991; Whalley *et al.* 1993). In none of these cases has the mechanism underlying mechanosensitivity been fully elucidated. Carrier phosphorylation appears to be involved in the response of NKCC1 to hyperosmolarity, although the kinases involved have not been identified (Haas & Forbush, 1998). NHE1 activity in isolated patches remains mechanosensitive in the absence of ATP, ruling out a phosphorylation mechanism for this transporter (Fuster *et al.* 2004). Cytoskeletal interactions (Venosa, 2003) and tyrosine phosphorylation (Bewick *et al.* 1999) have been implicated in the mechanosensitivity of the  $\text{Na}^+, \text{K}^+$ -ATPase, but are probably not involved in the case of NHE1 (Fuster *et al.* 2004).

In this report, we present evidence that the  $\text{Na}^+-\text{Ca}^{2+}$  exchanger is a mechanosensitive transporter and is stimulated by fluid flow and by hypotonicity. The exchanger is found in the plasma membrane of many cells, but is especially well expressed in excitable cells such as cardiac myocytes, where it is primarily responsible for mediating  $\text{Ca}^{2+}$  efflux. The exchanger couples  $\text{Ca}^{2+}$  efflux to the inward movement of  $\text{Na}^+$  ions. The stoichiometry is generally accepted to be  $3\text{Na}^+ : 1\text{Ca}^{2+}$  (Reeves & Hale, 1984), although there have been recent reports of higher values (Fujioka *et al.* 2000; Dong *et al.* 2002; Kang & Hilgemann, 2004). The exchanger can also operate in the reverse mode, moving  $\text{Ca}^{2+}$  into the cell when the normal thermodynamic gradients are altered, for example, by increasing cytosolic  $[\text{Na}^+]$  or reducing extracellular  $[\text{Na}^+]$ .

Wright *et al.* (1995) reported that NCX currents decreased by 40% when guinea pig cardiac myocytes were exposed to a hypotonic medium. The response to hypotonicity was time dependent, and gradually developed over a period of several minutes. Hypertonicity elicited a more complicated response, producing an increase in current magnitude that tended to be transient at osmolarities greater than 150% of isotonic, subsequently declining to below isotonic current levels.

In this report, we show that NCX activity, measured using fluorescent probe techniques, is stimulated by the mechanical effects associated with superfusion of solutions. Our results also show that NCX activity responds to osmotic stimuli, although in the direction opposite to that described by Wright *et al.* (1995).

## Methods

### Cells

CHO T cells (Chinese hamster ovary K1 cells expressing the human insulin receptor (Langille *et al.* 1999), kindly provided by Dr Michael Czech (University of Massachusetts Medical Ctr., Worcester, MA, USA)), were stably transfected with the mammalian expression vector pcDNA3 containing the coding sequence for the canine cardiac  $\text{Na}^+-\text{Ca}^{2+}$  exchanger (NCX1.1) or a deletion mutant,  $\Delta(241-680)$ . The  $\Delta(241-680)$  mutant is unregulated; it does not require allosteric activation by cytosolic  $\text{Ca}^{2+}$  and is resistant to an inactivation process induced by high cytosolic  $[\text{Na}^+]$  ( $\text{Na}^+$ -dependent inactivation) (Matsuoka *et al.* 1993). It was used for most of the experiments reported here in order to eliminate possible regulatory effects. However, it is important to note that the wild-type exchanger displayed the same mechanosensitive properties as the  $\Delta(241-680)$  mutant. In this report, we will occasionally refer to cells expressing the wild-type and mutant exchangers as 'wild-type cells' or ' $\Delta(241-680)$  cells'. 'Non-transfected cells' refers to the CHO T cells that were not transfected to express NCX; however, as stated above, they had previously been transfected to stably express the human insulin receptor (Langille *et al.* 1999). NCX activity in transfected CHO T cells is higher than in other CHO cell lines; the reasons for this enhanced expression are unknown. All cells were grown in F-12 medium supplemented with 10% fetal bovine serum, 2 mM L-glutamine, 100 U ml<sup>-1</sup> penicillin, 100  $\mu\text{g}$  ml<sup>-1</sup> streptomycin and 20  $\mu\text{g}$  ml<sup>-1</sup> gentamicin.

Neonatal rat myocytes were prepared as described previously (Abdellatif *et al.* 1994). Briefly, neonatal Sprague-Dawley rats (1 day old) were killed by cervical dislocation under an approved Institutional Animal Care and Use Committee (IACUC) protocol that conforms to the NIH animal welfare guidelines. The animals were then immediately dipped in 70% ethanol, placed on a dissecting board where an incision was made alongside the left edge of the sternum; pressure was applied on both sides of the incision, allowing the heart to pop out where it is accessible for dissection. Cells were dissociated using collagenase type II (Worthington), after which they were subjected to Percoll gradient centrifugation, followed by 30 min of differential pre-plating, to eliminate non-myocyte cells. Myocytes were cultured on fibronectin-coated plates in 1 : 1 Dulbecco's modified Eagle's medium : Ham F12 with 10% fetal bovine serum at a density of  $0.5-1 \times 10^5$  cells cm<sup>-2</sup>.

### Solutions

Na-PSS contained 140 mM NaCl, 5 mM KCl, 1 mM  $\text{MgCl}_2$ , 10 mM glucose and 20 mM 3-(*N*-morpholino)propanesulphonic acid (Mops), buffered to

pH 7.4 with Tris. The composition of K-PSS was similar except that NaCl was absent and the total concentration of KCl was 140 mM. Solutions designated 20/120 or 100/40 Na/K-PSS contained the indicated concentrations of Na<sup>+</sup> and K<sup>+</sup> (e.g. 20 mM NaCl + 120 mM KCl, etc.) plus 1 mM MgCl<sub>2</sub>, 10 mM glucose and 20 mM Mops/Tris, pH 7.4; 70 Na-PSS contained 70 mM NaCl plus 1 mM MgCl<sub>2</sub>, 10 mM glucose and 20 mM Mops/Tris, pH 7.4. For the osmolarity studies we used solutions containing mannitol, designated 70/140 or 70/500 Na/mannitol-PSS, which contained 70 mM NaCl and either 140 or 500 mM mannitol plus 1 mM MgCl<sub>2</sub>, 10 mM glucose and 20 mM Mops/Tris, pH 7.4. The osmolarities of 70 Na-PSS, 70/140 Na/manitol-PSS and 70/500 Na/mannitol-PSS were 185, 333 and 768 mosmol (kg H<sub>2</sub>O)<sup>-1</sup>, respectively. Biochemicals were purchased from Sigma, unless indicated otherwise, and cell culture media, including fetal bovine serum, was from Life Technologies. Fura-2 AM and calcein-AM were obtained from Molecular Probes.

### Fura-2 imaging

Cells were grown on 25 mm circular coverslips and loaded with fura-2 by incubating the coverslips for 30–40 min at room temperature in Na-PSS containing 1 mM CaCl<sub>2</sub>, 0.25 mM sulfonpyrazone (to retard fura-2 transport from the cell) and 3 μM fura-2 AM. The coverslips were then washed in Na-PSS + 1 mM CaCl<sub>2</sub>, placed in a stainless steel holder (bath volume ~0.8 ml; Molecular Probes), and viewed in a Zeiss Axiovert 100 microscope coupled to an Attofluor digital imaging system. Forty to sixty individual cells were selected and monitored simultaneously as 8 pixel × 8 pixel regions of interest for each coverslip. At the end of each experiment, 10 mM MnCl<sub>2</sub> was added along with ionomycin (1 μM) to quench fura-2 fluorescence and determine background fluorescence levels. Results are presented as the ratio (*R*) of fluorescence intensities, after correction for background emission, at excitation wavelengths of 334 nm (350 nm for Ba<sup>2+</sup>) and 380 nm (390 nm for Ba<sup>2+</sup>). Emission was monitored at > 510 nm. Each trace presented in the figures reflects the mean response of 40–60 cells on an individual coverslip or the average of multiple coverslips. In figures where a trace from a single coverslip is shown, the experiment is representative of similar results obtained on three or more occasions, with minor variations in time of the solution applications.

### Measurement of NCX activity

Most experiments used the monovalent cation channel-forming ionophore gramicidin to clamp cytosolic [Na<sup>+</sup>] at the desired level. Unless otherwise specified, cells were placed in Na-PSS containing 0.3 mM EGTA approximately 10 min before beginning the recordings and Ca<sup>2+</sup> was released from the endoplasmic reticulum by applying 100 μM ATP + 2 μM thapsigargin (Tg), an irreversible and

selective inhibitor of the sarco(endo)plasmic reticulum Ca<sup>2+</sup> ATPase (SERCA; Lytton *et al.* 1991). Approximately 8 min before beginning the recordings, the coverslip was washed with 5 ml of the desired Na/K-PSS solution containing 0.3 mM EGTA and 1 ml of the same solution containing 1 μg ml<sup>-1</sup> gramicidin was then added. Occasional departures from this protocol are fully described in the text.

To initiate the Ca<sup>2+</sup> influx ('reverse') mode of NCX activity, either 0.1 mM CaCl<sub>2</sub> or the desired concentration of BaCl<sub>2</sub> in the Na/K-PSS solution used for the pre-incubation with gramicidin was applied to the cells. The Ba<sup>2+</sup> solutions also contained 0.1 mM EGTA to chelate contaminating Ca<sup>2+</sup>. Two methods of solution change were employed. First, as in our previous publications, we used a syringe to manually superfuse 4–5 ml of the assay medium with continuous aspiration of excess solution (superfusion protocol). We measured the solution mixing time using this approach as follows: we applied 5 ml of Na-PSS + 0.3 mM EGTA to a coverslip holder containing 0.8 ml of a 5 μM solution of fura-2 (free acid) in Na-PSS + 0.3 mM EGTA. The mean time constant (± s.e.m., *n* = 3) for the decline in the fluorescence during the solution flow was 1.89 ± 0.17 s. In the second approach, we quickly removed the pre-incubation medium by aspiration and replaced it with 1 ml of assay medium (rapid replacement protocol). This exchange of solutions takes 2–3 s. All experiments were carried out at 37°C.

Similar approaches were used to measure NCX activity in neonatal cardiac myocytes, except that it was necessary to use La<sup>3+</sup> instead of Ca<sup>2+</sup> or Ba<sup>2+</sup> because of Ca<sup>2+</sup> channel activity (Reeves & Condrescu, 2003). Cells were treated with 10 mM caffeine plus 2 μM Tg 10 min prior to recording to remove Ca<sup>2+</sup> from the sarcoplasmic reticulum. The cells were then treated with 1 μg ml<sup>-1</sup> gramicidin in 100/40 Na/K-PSS containing 30 μM EGTA. Exchange activity was initiated by applying 20 μM LaCl<sub>3</sub> in 100/40 Na/K-PSS, using either the superfusion or rapid replacement protocols. The ratios were not corrected for background fluorescence because Mn<sup>2+</sup> did not completely quench fura-2 fluorescence in the presence of La<sup>3+</sup>.

## Results

### Ca<sup>2+</sup> uptake by reverse mode NCX activity in transfected CHO cells

During Ca<sup>2+</sup> uptake by reverse-mode NCX activity, cytosolic [Ca<sup>2+</sup>] typically rises to a peak and then declines toward a steady-state value. This is illustrated by the data in Fig. 1, in which fura-2-loaded cells expressing the 'non-regulated' NCX deletion mutant, Δ(241–680), were preincubated with the monovalent cation ionophore

gramicidin in either 10/130 Na/K-PSS or 100/40 Na/K-PSS (see Methods).  $\text{Ca}^{2+}$  influx was initiated by superfusing 5 ml of either 10/130 or 100/40 Na/K-PSS containing 0.1 mM  $\text{Ca}^{2+}$ , as indicated. The rate of  $\text{Ca}^{2+}$  uptake was somewhat less in the 10/130 Na/K-PSS medium, but in both cases, the fura-2 ratio increased to a peak value in 30–40 s and then declined to a steady-state value over the next several minutes.

The post-peak decline in  $[\text{Ca}^{2+}]_i$  cannot be attributed to a loss of cytosolic  $\text{Na}^+$  since  $\text{Na}^+$  influx through the gramicidin channels keeps  $[\text{Na}^+]_i$  constant. We reported previously that the post-peak decline in the fura-2 ratio could be greatly reduced or eliminated by treating the cells with mitochondrial uncouplers (Opuni & Reeves, 2000; Urbanczyk *et al.* 2006). However, post-peak declines can be observed even in the presence of uncouplers, although the decline occurs more slowly than in their absence (data not shown). Although mitochondrial  $\text{Ca}^{2+}$  accumulation undoubtedly contributes to the decline in  $[\text{Ca}^{2+}]_i$  in the experiments shown in Fig. 1, the results described below indicate that there is also a fall-off in NCX activity itself following the initiation of  $\text{Ca}^{2+}$  influx.

### Biphasic $\text{Ba}^{2+}$ uptake by NCX

We have often used  $\text{Ba}^{2+}$  as a surrogate for  $\text{Ca}^{2+}$  to measure reverse-mode NCX activity (Condrescu *et al.* 1997). Some of the advantages of using  $\text{Ba}^{2+}$  are that it is not transported by SERCA or the plasma membrane  $\text{Ca}^{2+}$  ATPase and it is not extensively taken up by mitochondria.

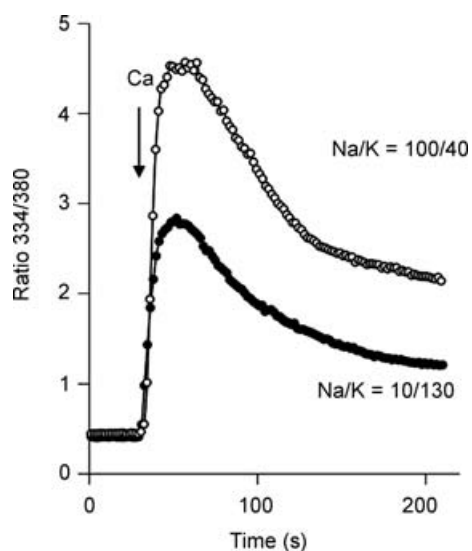


**Figure 1.**  $\text{Ca}^{2+}$  uptake by CHO cells expressing the  $\Delta(241\text{--}680)$  mutant of NCX

Cells were pre-treated with ATP + Tg, and with  $1 \mu\text{g ml}^{-1}$  gramicidin in either 10/130 or 100/40 Na/K-PSS containing 0.3 mM EGTA as described in Methods.  $\text{Ca}^{2+}$  uptake was initiated by superfusing 4–5 ml of 0.1 mM  $\text{Ca}^{2+}$  in 10/130 or 100/40 Na/K-PSS. The results are representative of experiments conducted on more than 3 separate occasions.

Thus,  $\text{Ba}^{2+}$  uptake experiments are less complicated by organellar sequestration or efflux activity than  $\text{Ca}^{2+}$  uptake experiments. The data in Fig. 2 show that the time course of  $\text{Ba}^{2+}$  uptake is markedly dependent upon the procedure used to initiate NCX activity. In Fig. 2A, cells expressing the wild-type NCX were treated with gramicidin in 100/40 Na/K-PSS containing 0.3 mM EGTA (see Methods). Reverse-mode NCX activity was then initiated by applying 2 mM  $\text{Ba}^{2+}$  in 100/40 Na/K-PSS. In trace *a* in Fig. 2A (open circles), a 5 ml volume of the 2 mM  $\text{Ba}^{2+}$  solution was superfused over a 20 s interval; the duration of the superfusion period is indicated by the bar beneath the trace.  $\text{Ba}^{2+}$  influx was a biphasic process under these conditions, showing an initial rate of  $\text{Ba}^{2+}$  uptake that in this instance was more than 13 times greater than the rate of  $\text{Ba}^{2+}$  entry seen after 250 s. In trace *b*, we used a different procedure to initiate  $\text{Ba}^{2+}$  uptake: the preincubation solution (0.8 ml) was rapidly aspirated and replaced with 1 ml of the 2 mM  $\text{Ba}^{2+}$  solution. As shown, the initial rapid phase of  $\text{Ba}^{2+}$  influx was nearly eliminated under these conditions and  $\text{Ba}^{2+}$  uptake over the remainder of the experiment paralleled the slow phase of  $\text{Ba}^{2+}$  influx seen in trace *a*.

For the results shown in Fig. 2B, the approach was similar to that described above except that cells expressing the  $\Delta(241\text{--}680)$  mutant were used and the gramicidin-treated cells were equilibrated with a lower  $\text{Na}^+$  concentration (20/120 Na/K-PSS). The rates of  $\text{Ba}^{2+}$  influx were higher under these conditions than for the experiment shown in Fig. 2A, mainly because of the reduced competition by  $\text{Na}^+$  for  $\text{Ba}^{2+}$  binding to the extracellular translocation sites. Again, there was a profound difference between the two methods of solution change. Thus, superfusing 5 ml of the  $\text{Ba}^{2+}$  solution over a 20 s interval (trace *a*) resulted in the rapid uptake of  $\text{Ba}^{2+}$  to a maximal value. For the rapid replacement procedure, where the preincubation solution was removed and quickly replaced with 1 ml of the  $\text{Ba}^{2+}$  solution (trace *b*), the rapid phase of  $\text{Ba}^{2+}$  influx was greatly attenuated. At the arrow labelled 'R' in trace *b*, the cells were superfused with a 5 ml volume of the  $\text{Ba}^{2+}$  solution over a 20 s interval, and a sharp increase in  $\text{Ba}^{2+}$  influx was observed. Note that there was no change in the ionic conditions during the second application: the composition of re-applied solution was identical to the solution applied initially. The results indicate that  $\text{Ba}^{2+}$  uptake during the slow phase can be re-activated simply by re-initiating solution flow.

$\text{Ba}^{2+}$  uptake under these conditions is due solely to NCX activity, as shown by trace *c* in Fig. 2B, which displays the results of identical experiments carried out with non-transfected CHO T cells.  $\text{Ba}^{2+}$  uptake was extremely low and was unaffected by the method used to apply the  $\text{Ba}^{2+}$  solutions; the trace reflects the average of three experiments carried out with the superfusion procedure and two experiments with the rapid replacement procedure.

We next asked whether other modes of  $Ba^{2+}$  entry would exhibit a similar dependence upon solution flow. For this purpose, we measured  $Ba^{2+}$  uptake through store-operated channels using non-transfected CHO T cells; since gramicidin strongly depolarizes the cell membrane, thereby inhibiting store-operated channel activity, we omitted gramicidin in these experiments. In Fig. 2C, internal  $Ca^{2+}$  stores were depleted with ATP + Tg as usual (see Methods) and the cells were preincubated for 10 min in Na-PSS + 0.3 mM EGTA without gramicidin.  $Ba^{2+}$  uptake was then initiated by applying 2 mM  $BaCl_2$  in Na-PSS using either the 5 ml superfusion procedure (trace *a*) or the rapid replacement procedure (trace *b*). The results show a modest increase in  $Ba^{2+}$  uptake for the superfusion procedure compared to the rapid replacement procedure, and only a small stimulation when 5 ml of the  $Ba^{2+}$  solution was re-applied (R). Thus,  $Ba^{2+}$  influx through store-operated channels exhibits a small degree of stimulation by superfusion, but the results are much less pronounced than for NCX activity.

For the superfusion procedure, 95% of the solution exchange occurred in less than 6 s (see Methods), so that more than two thirds of the 20 s duration of superfusion occurred after the solution exchange was complete. For the rapid replacement protocol, the solution change occurred in 3 s or less. The data presented below suggest that the duration of solution flow is the primary determinant of the amplitude of the rapid phase of  $Ba^{2+}$  uptake, and that NCX activity is stimulated by the mechanical effects associated with solution flow. For the results shown in Fig. 3, cells expressing the  $\Delta(241-680)$  mutant were treated with gramicidin and equilibrated with 20/120 Na/K-PSS. Exchange activity was initiated by applying 0.5 mM  $Ba^{2+}$  in 20/120 Na/K-PSS. The lower  $Ba^{2+}$  concentration was chosen so that the fura signal would not become saturated during the rapid phase of uptake. In trace *a*, the rapid replacement procedure was used to initiate  $Ba^{2+}$  influx. For trace *b*, 4 ml of the 0.5 mM  $Ba^{2+}$  solution was superfused over a 15 s period, as indicated by the bar labelled 'b' below the trace. The rapid phase was greatly increased

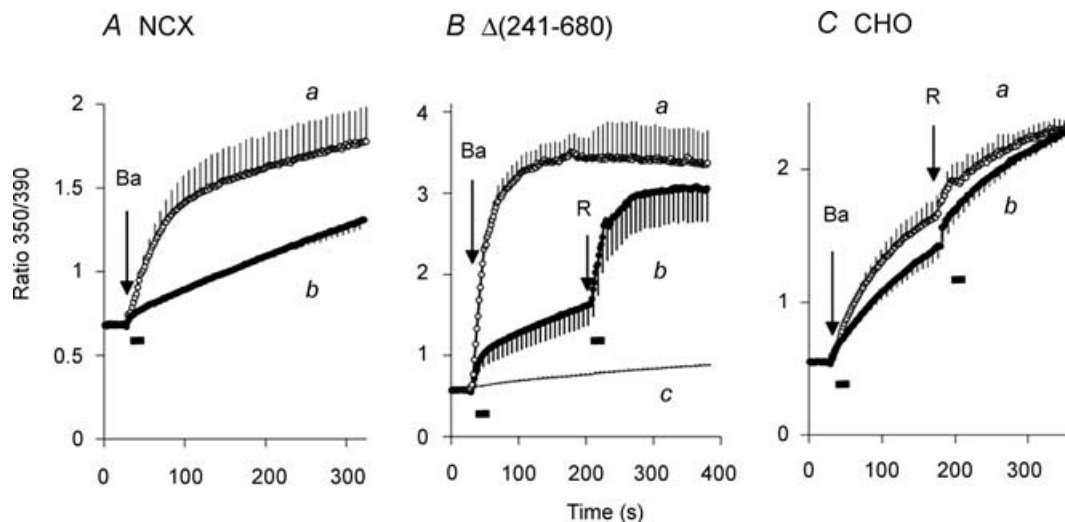


**Figure 2.**  $Ba^{2+}$  uptake by CHO cells expressing either the wild-type NCX1.1 (A) or the  $\Delta(241-680)$  mutant (B), or by non-transfected CHO T cells (C)

A, after releasing internal  $Ca^{2+}$  stores with ATP + Tg (see Methods), cells expressing the wild-type NCX1.1 were treated with  $1 \mu\text{g ml}^{-1}$  gramicidin and pre-equilibrated in 100/40 Na/K-PSS.  $Ba^{2+}$  uptake was initiated by applying 2 mM  $Ba^{2+}$  in 100/40 Na/K-PSS containing 0.1 mM EGTA to chelate contaminating  $Ca^{2+}$ . In trace *a*, 5 ml of the assay solution was superfused with continuous aspiration, while in trace *b*, the pre-equilibration was removed and quickly replaced with 1 ml of the assay medium. Traces represent the mean values ( $\pm$  s.e.m.) of 3 (trace *a*) or 5 (trace *b*) coverslips; error bars are shown for every fourth data point. B, gramicidin-treated CHO cells expressing the  $\Delta(241-680)$  mutant of NCX were pre-equilibrated in 20/120 Na/K-PSS.  $Ba^{2+}$  uptake was initiated by superfusion of 5 ml of 2 mM  $Ba^{2+}$  in 20/120 Na/K-PSS (trace *a*,  $n = 4$  coverslips) or by removing the pre-equilibration medium and replacing it with 1 ml of the assay medium (trace *b*,  $n = 3$ ). For trace *b*, at the arrow labelled R, an additional 5 ml of 2 mM  $Ba^{2+}$  in 20/120 Na/K-PSS was applied by superfusion. For trace *c*, non-transfected CHO T cells were treated with gramicidin and assayed for Ba uptake under the conditions used for cells expressing the  $\Delta(241-680)$  mutant. The trace represents the average of 3 experiments carried out by superfusing 5 ml of the  $Ba^{2+}$  solution and 2 experiments using the rapid replacement method. For the latter traces, an additional 5 ml of  $Ba^{2+}$  solution was superfused at the time indicated by the arrow labelled R. C, after depleting internal  $Ca^{2+}$  stores with ATP + Tg, non-transfected CHO T cells were pre-incubated for 10 min in Na-PSS + 0.3 mM EGTA without added gramicidin.  $Ba^{2+}$  uptake was measured in non-transfected CHO cells by superfusing 5 ml of 2 mM  $BaCl_2$  in Na-PSS (trace *a*,  $n = 3$ ) or by rapidly replacing the pre-incubation medium with 1 ml of 2 mM  $BaCl_2$  in Na-PSS (trace *b*,  $n = 3$ ). At the arrow labelled R, an additional 5 ml of the  $Ba^{2+}$  solution was applied by superfusion for both traces. The bars beneath the traces represent the time during which the 5 ml of solution were applied.

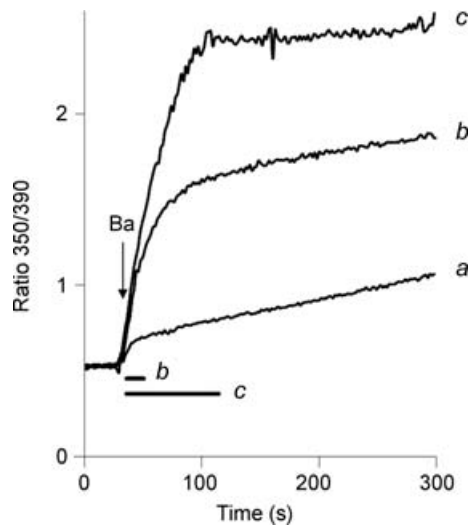


**Figure 3. Duration of solution changes and stimulation of  $\text{Ba}^{2+}$  uptake**

Gramicidin-treated cells expressing the  $\Delta(241-680)$  mutant of NCX were equilibrated in 20/120 Na/K-PSS. NCX activity was initiated by superfusing 4 ml (trace *b*) or 20 ml (trace *c*) of 0.5 mM  $\text{Ba}^{2+}$  in 20/120 Na/K-PSS over durations of 15 s and 80 s, respectively, as shown by the bars labelled '*b*' and '*c*' below the traces. For trace *a*,  $\text{Ba}^{2+}$  influx was initiated by the rapid replacement procedure. This experiment, or similar variants of it, was repeated more than 3 times with similar results.

in amplitude compared to trace *a*. For trace *c*, 20 ml of the  $\text{Ba}^{2+}$  solution was superfused over an 80 s interval (see bar labelled '*c*'). In this case,  $\text{Ba}^{2+}$  influx continued at a rapid rate during the entire period in which solution was

being applied and effectively ceased once the solution flow ended.

Repeated superfusions of 4 ml volumes of  $\text{Ba}^{2+}$  or  $\text{Ca}^{2+}$  solutions produced repeated enhancements of reverse-mode NCX activity. In Fig. 4A,  $\Delta(241-680)$  cells were pre-treated with gramicidin in 20/120 Na/K-PSS. At point *a*, a 4 ml volume of 0.5 mM  $\text{Ba}^{2+}$  in 20/120 Na/K-PSS was applied by superfusion to initiate NCX activity. As in the previously described figures,  $\text{Ba}^{2+}$  influx was bi-phasic. At *b*, a second 4 ml volume of the same 0.5 mM  $\text{Ba}^{2+}$  solution was superfused and an additional rapid phase of  $\text{Ba}^{2+}$  influx was observed, followed by a period in which  $\text{Ba}^{2+}$  influx appeared to cease. At *c*, a third 4 ml volume of the 0.5 mM  $\text{Ba}^{2+}$  solution was superfused. Again there was a rapid increase in  $\text{Ba}^{2+}$  uptake, although the effect was smaller than the previous two trials. At *d*, 4 ml of 20/120 Na/K-PSS containing 5 mM  $\text{Ba}^{2+}$  was superfused; the large increase in  $\text{Ba}^{2+}$  influx demonstrates that the fura-2 signal was not saturated after the previous addition. Finally, at *e*, 20/120 Na/K-PSS containing 0.3 mM EGTA was applied, after which a gradual decline in the fura-2 signal was seen, suggesting that  $\text{Ba}^{2+}$  efflux was occurring under these conditions.

Figure 4B displays data from  $\Delta(241-680)$  cells pre-treated with gramicidin in 100/40 Na/K-PSS. In this case, NCX activity was initiated (at point *a*) by superfusing 3–4 ml of 0.1 mM  $\text{Ca}^{2+}$  (instead of  $\text{Ba}^{2+}$ ) in 100/40 Na/K-PSS. Like the results in Fig. 1,  $[\text{Ca}^{2+}]_i$  increased rapidly toward a peak and subsequently declined to a steady-state value. At *b*, another 3–4 ml volume of the

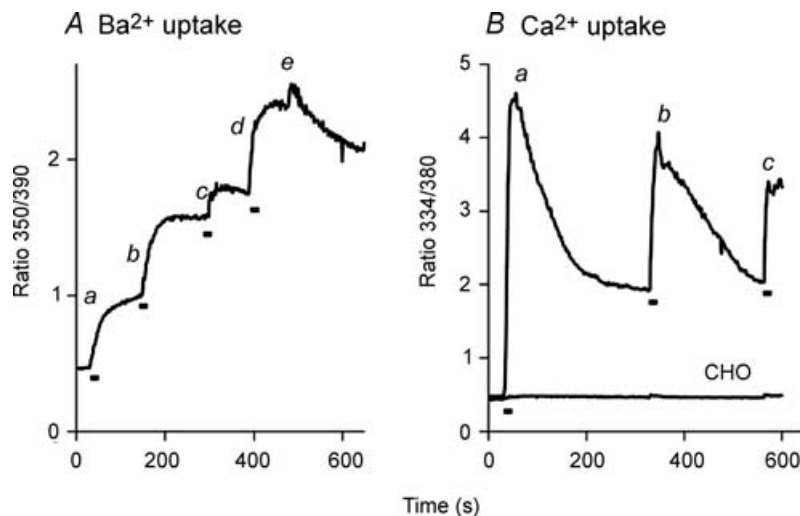


**Figure 4. Multiple stimulations of  $\text{Ba}^{2+}$  (A) and  $\text{Ca}^{2+}$  (B) uptake by repeated solution applications**

A, gramicidin-treated cells expressing the  $\Delta(241-680)$  NCX mutant were equilibrated in 100/40 Na/K-PSS. The labelled points designate the superfusion of 4 ml of 2 mM  $\text{Ba}^{2+}$  in 100/40 Na/K-PSS (*a*, *b*, *c*), 5 mM  $\text{Ba}^{2+}$  in 20/120 Na/K-PSS (*d*) or 0.3 mM EGTA in 20/120 Na/K-PSS (*e*). B, gramicidin-treated  $\Delta(241-680)$  cells were equilibrated in 100/40 Na/K-PSS. Five millilitres of 100/40 Na/K-PSS containing 0.1 mM  $\text{Ca}^{2+}$  were applied by superfusion at points *a*, *b* and *c*. Bars beneath traces depict duration of the superfusions. This experiment was repeated, with minor variations, more than 3 times with similar results. The trace labelled 'CHO' represents an identical experiment carried out with non-transfected CHO T cells; the experiment with the non-transfected cells was repeated on 2 additional occasions with identical results.

same 0.1 mM Ca<sup>2+</sup> solution was superfused and [Ca<sup>2+</sup>]<sub>i</sub> again rose rapidly to a peak, which was not quite as high as the first peak, and then declined again. At *c*, a third volume of 0.1 mM Ca<sup>2+</sup> solution was superfused and again a rapid increase in [Ca<sup>2+</sup>]<sub>i</sub> was observed. The results with Ca<sup>2+</sup> are analogous to those with Ba<sup>2+</sup>, leading us to conclude that NCX activity is stimulated during periods in which solution flow occurs, and declines during the interflow periods. As a control, identical experiments were conducted with non-transfected CHO T cells and the results are shown by the trace labelled 'CHO' in Fig. 4B. No Ca<sup>2+</sup> uptake was observed under these conditions, and re-application of the assay medium at points *b* and *c* did not significantly affect the trace.

**Flow-dependent stimulation of Ba<sup>2+</sup> efflux and Ca<sup>2+</sup>-Ba<sup>2+</sup> exchange**

To determine whether solution flow stimulated the forward mode of NCX activity as well as the reverse mode, we examined NCX-mediated Ba<sup>2+</sup> efflux. In the

experiment in Fig. 5A, Δ(241–680) cells (in this case, *not* treated with gramicidin) were allowed to accumulate Ba<sup>2+</sup> by reverse-mode NCX activity in K-PSS. At point *a*, Ba<sup>2+</sup> uptake was stopped by applying K-PSS containing 0.3 mM EGTA. There was a brief transient rise in the fura-2 ratio, which is due to a solution-change artifact (see below). Following the transient increase, there was a slow decline in the ratio. Superfusion of 5 ml of Na-PSS (point *b*) induced rapid Ba<sup>2+</sup> efflux, but this was followed by a period of slower Ba<sup>2+</sup> efflux. Superfusion of a second 5 ml volume of Na-PSS at point *c* substantially increased the rate of Ba<sup>2+</sup> efflux for 40–60 s. The rates of Ba<sup>2+</sup> efflux, given as the negative slopes of the trace over time intervals 1–5 (see labelled bars beneath the trace) are presented in Fig. 5D; the slopes have been multiplied by –1 to simplify presentation. As shown for the rates from the data in panel A (open bars), the rate of Ba<sup>2+</sup> efflux increased markedly during the superfusion of Na-PSS (intervals 2 and 4) but subsequently declined following termination of the superfusion (intervals 3 and 5).

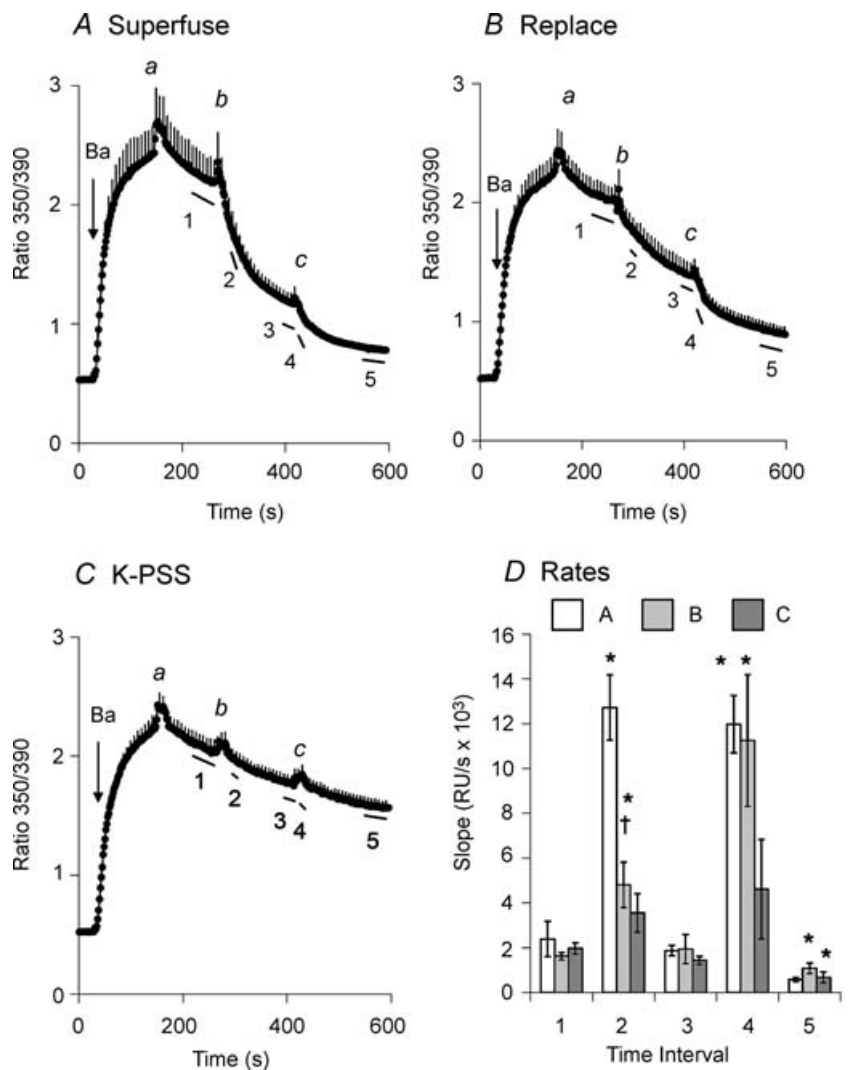


**Figure 5. Flow-dependent stimulation of the forward mode of NCX activity**  
 A, cells expressing Δ(241–680) were pre-treated with ATP + Tg in Na-PSS + 0.3 mM EGTA; gramicidin was not used in these experiments. Ba<sup>2+</sup> uptake was initiated by applying 1 mM Ba<sup>2+</sup> in K-PSS. The labelled points designate the superfusion of 5 ml of 0.3 mM EGTA in K-PSS (*a*) or Na-PSS (*b*, *c*). Error bars are shown for every fourth data point (*n* = 5). B, experimental conditions as in A. The labelled points designate the superfusion of 5 ml of 0.3 mM EGTA in K-PSS (*a*) or Na-PSS (*c*), or, for *b*, the removal of 0.3 mM EGTA in K-PSS and its rapid replacement with 1 ml of 0.3 mM EGTA in Na-PSS (*n* = 4). C, experimental conditions as in A. The labelled points designate the repeated superfusions of 5 ml of 0.3 mM EGTA in K-PSS (*n* = 4). D, slopes of the traces over the time intervals designated by the lines beneath the traces labelled 1–5 in panels A–C. \* *P* < 0.05 versus slope at time interval 1. † *P* < 0.05 for data at time interval 2 for superfusion (A) versus rapid replacement (B).

Figure 5B shows an identical experiment to that shown in Fig. 5A, except that  $Ba^{2+}$  efflux was initiated at point *b* by the rapid replacement procedure instead of superfusion. The rate of  $Ba^{2+}$  efflux increased significantly, as shown by the lightly shaded bar in panel *D* at interval 2, but was substantially less than that produced by superfusion (compare with open bar). After superfusing 5 ml of the Na-PSS at point *c* (panel *B*) the rate of  $Ba^{2+}$  efflux increased transiently to become equal to the rate shown in panel *A* (compare lightly shaded and open bars at interval 4 in panel *D*).

Figure 5C shows the results of a control experiment in which K-PSS was superfused at points *b* and *c* instead of Na-PSS. In each case, there was a small, transient increase in the fura-2 ratio followed by a slow decline. No stimulation of Ba efflux was observed upon superfusion of the K-PSS, although the slopes given by the darkly shaded bars in Fig. 5D show small, non-significant increases at intervals 2 and 4 which clearly reflect the recovery of the fura ratio from the solution exchange artifact (see below). Thus, the rapid fall in the fura ratio in panels *A* and *B* reflects NCX-mediated  $Ba^{2+}$  efflux; the difference in behaviour between the rapid replacement and the superfusion procedures is analogous to that seen for reverse-mode  $Ba^{2+}$  uptake. We conclude that both the forward and reverse modes of NCX activity were stimulated during the periods in which solution flow occurred.

The data in Fig. 6 show that flow-dependent stimulation also occurred when the exchanger operated in a  $Ca^{2+}$ - $Ca^{2+}$  exchange mode, as determined by measuring  $Ca^{2+}$ - $Ba^{2+}$  exchange in the absence of  $Na^+$  ions. For this purpose,  $\Delta(241-680)$  cells were treated with ATP to release  $Ca^{2+}$  from internal stores, but in contrast to our usual procedure, Tg was not included so that SERCA could remain active throughout the experiment. The cells were equilibrated with 20/120 Na/K-PSS in the presence of gramicidin.  $Ba^{2+}$  influx was initiated by applying 1 mM  $Ba^{2+}$  in K-PSS and was terminated after 2 min (point *a*) by applying K-PSS + 0.3 mM EGTA. In the  $Na^+$ -free medium,  $Na^+$  ions would be expected to leave the cell rapidly through the gramicidin channels.  $Ca^{2+}$ - $Ba^{2+}$  exchange was initiated at point *b* by applying 0.1 mM  $Ca^{2+}$  in K-PSS, using either the superfusion procedure (panel *A*) or the rapid replacement procedure (panel *B*). In panel *A*, a steep decline in the fura-2 signal at point *b* was due to  $Ba^{2+}$  efflux in exchange for extracellular  $Ca^{2+}$ . The  $Ca^{2+}$  entering the cell in exchange for  $Ba^{2+}$  was rapidly accumulated in the endoplasmic reticulum by SERCA activity and was therefore not registered in the fura-2 signal. When  $Ca^{2+}$ - $Ba^{2+}$  exchange was initiated by the rapid replacement procedure (Fig. 6B), the decline in the fura signal was not as steep as for the superfusion procedure. The rates of  $Ba^{2+}$  efflux, given as the negative slope of the traces over time interval 2 (Fig. 6C), are significantly different for the two procedures. At point *c* in both panels, an additional 5 ml

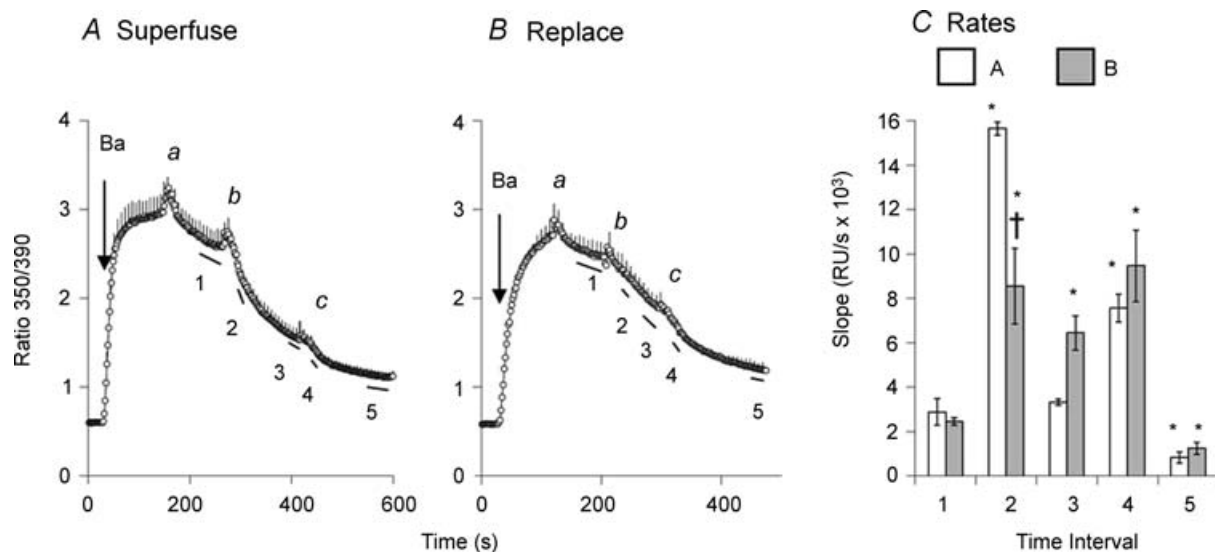


**Figure 6. Flow-dependent stimulation of  $Ca^{2+}$ - $Ba^{2+}$  exchange**

*A*, cells expressing  $\Delta(241-680)$  were treated with ATP (without Tg) approximately 10 min before beginning the recordings to release  $Ca^{2+}$  from the ER. At 8 min before recording, cells were treated with gramicidin in 20/120 Na/K-PSS.  $Ba^{2+}$  uptake was initiated by applying 1 mM  $Ba^{2+}$  in K-PSS. The labelled points designate the superfusion of 5 ml of K-PSS containing 0.3 mM EGTA (*a*) or 0.1 mM  $Ca^{2+}$  (*b*, *c*). Error bars are shown for every fourth data point ( $n = 3$ ). *B*, the experiment follows the same procedure described in *A* except that at point *b*, the 0.1 mM  $Ca^{2+}$  solution was applied by the rapid replacement procedure ( $n = 3$ ). *C*, slopes of the traces over the intervals designated by the lines beneath the traces labelled 1–5 in panels *A* and *B*, as indicated. \* $P < 0.05$  versus slope at time interval 1. † $P < 0.05$  for data at time interval 2 for superfusion (*A*) versus rapid replacement (*B*).

of the the 0.1 mM  $\text{Ca}^{2+}$  solution was applied by superfusion. The rates of  $\text{Ba}^{2+}$  efflux (Fig. 6C) are in general similar to those for forward mode NCX activity (Fig. 5D), except that the stimulation of efflux produced by the second superfusion at point *c* (time interval 4) was not as pronounced.

### Flow- and volume-dependent changes in fura-2 fluorescence

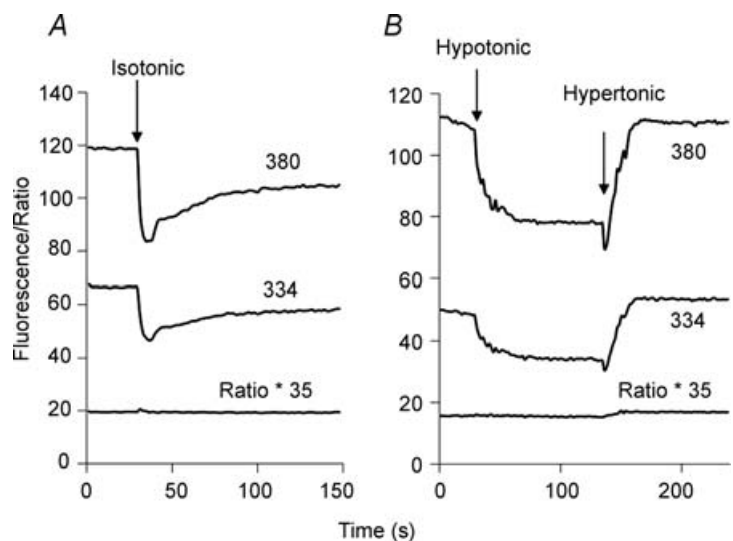
The data in Fig. 7 show that superfusion of cells was associated with changes in the fura-2 fluorescence intensities at both 334 nm and 380 nm. Here, fura-2-loaded  $\Delta(241-680)$  cells were treated with gramicidin in 20/120 Na/K-PSS and the fluorescence intensities (emission 510 nm) at 334 and 380 nm excitation were monitored during superfusion of 5 ml of the pre-incubation solution, i.e. 20/120 Na/K-PSS containing 0.3 mM EGTA. There was a transient decline of about 30% in the fluorescence intensities at each wavelength during the superfusion, followed by a gradual, but in this case only partial, recovery when the solution flow was stopped. No release of fura-2 from the cells was detectable during solution flow (see online Supplemental material). The trace labelled 'Ratio \* 35' depicts the 334/380 ratio (after background subtraction) multiplied by a scaling factor of 35. No change in the ratio was observed despite the fall in the individual fluorescence intensities at the two wavelengths. At higher ratios, however, a transient increase in the fura-2 ratio was observed during solution flow, as illustrated in Figs 4 and 5. This probably occurs because at high ratios (high cytosolic  $[\text{Ba}^{2+}]$ ), the fluorescence at 390 nm excitation had declined substantially and was much closer to background intensity. Since the background-corrected fluorescence intensity at 390 nm comprises the denominator of the ratio, decreases in the 390 nm intensity can cause a transient increase in the ratio after background subtraction.

Longer-lasting changes in fluorescence intensities were produced by applying hypotonic or hypertonic solutions, as shown in Fig. 7B. The cells were initially placed in an isotonic solution (70/140 Na/mannitol-PSS), and then superfused with a hypotonic solution (70 Na-PSS). A decline in fluorescence intensities was again observed, but in this case, partial recovery did not occur after cessation of flow. Instead, there was a further decline in fluorescence intensity. No change in the fura-2 ratio was detectable. At the arrow labelled 'hypertonic', we applied 5 ml of 70/500 Na/mannitol-PSS by superfusion. In this case, there was a small initial drop in fluorescence (reflecting solution flow), and then a marked increase (due to cell shrinkage). There was also a small increase in the 334/380 ratio. These volume-dependent changes in the fura-2 fluorescence intensities are essentially the same as those described by Muallem *et al.* (1992).

The transient decline in fluorescence produced by superfusion of isotonic solution (Fig. 7A) suggested that, like the application of a hypotonic solution (Fig. 7B), the superfusion procedure might be inducing a volume increase. However, when we monitored calcein-loaded cells during superfusion by fluorescence microscopy, we could not detect an increase in cell volume, although volume changes were readily observed in the hypotonic and hypertonic media (see Supplemental material). In some cases, small displacements of the cells were noted during superfusion and this might be responsible for the decline in fluorescence intensity within the regions of interest that we monitor during fluorescence measurements (see Methods). A partial, but variable, loss of focus during solution flow also occurs, and this would likewise contribute to the reduction in fura-2 fluorescence intensities. Our evidence, however, suggests that no dramatic changes in cell volume or shape occur during solution superfusion. We could not detect any release of fura-2 from the cells during superfusion, although the low total fura-2 content of the coverslip would limit our ability

### Figure 7. Effect of solution applications and osmotic changes on fura-2 fluorescence intensities

**A**, gramicidin-treated cells expressing  $\Delta(241-680)$  were equilibrated in 20/120 Na/K-PSS containing 0.3 mM EGTA; at the arrow labelled 'Isotonic', 5 ml of 20/120 Na/K-PSS + 0.3 mM EGTA was applied. The fura-2 fluorescence intensities with 334 and 380 nm excitation, corrected for background, are depicted. The trace labelled 'Ratio \* 35' depicts the 334/380 ratio multiplied by a factor of 35 in order to scale to the figure. **B**, gramicidin-treated  $\Delta(241-680)$  cells were equilibrated with 70/70 Na/K-PSS containing 0.3 mM EGTA. Two minutes prior to beginning the recordings, the medium was changed to 70/140 Na/mannitol-PSS. The labelled arrows designate the application of 5 ml of 70 Na-PSS (Hypotonic) or 70/500 Na/mannitol-PSS (Hypertonic). These experiments have been repeated more than 3 times with similar results.



to detect small amounts of release (see Supplemental material).

### Volume-dependent changes in NCX activity

Mechanosensitivity of channels and transporters is often revealed when cells are subjected to osmotically induced volume changes. For  $\text{Na}^+$ – $\text{Ca}^{2+}$  exchange activity, osmotically induced volume changes may introduce difficulties in interpretation due to associated changes in cytosolic  $[\text{Na}^+]$  that would affect the driving force for NCX. We therefore chose to load cells with 70 mM  $\text{Na}^+$  using the gramicidin technique. This concentration is substantially higher than the  $K_D$  for cytosolic  $\text{Na}^+$  (17 mM; Matsuoka *et al.* 1993), so that kinetic effects associated with alterations in  $[\text{Na}^+]_i$  would be minimized. For the experiment shown in Fig. 8,  $\Delta(241\text{--}680)$  cells were equilibrated in 70/70 Na/K-PSS and, 2 min prior to recording, the medium was changed to 70/140 Na/mannitol-PSS. Exchange activity was then initiated by superfusing 0.1 mM  $\text{Ca}^{2+}$  in 5 ml of either an isotonic medium (70/140 Na/mannitol-PSS), a hypotonic medium (70 Na-PSS) or a hypertonic medium (70/500 Na/mannitol-PSS). As shown in Fig. 8A,  $\text{Ca}^{2+}$  uptake was stimulated in the hypotonic medium and inhibited in the hypertonic medium. The amplitudes of the  $[\text{Ca}^{2+}]_i$  peak

increased in the order hypertonic < isotonic < hypotonic; the rates and extents of the post-peak decline followed the opposite order. Initial rates of  $\text{Ca}^{2+}$  uptake also tended to increase in the order hypertonic < isotonic < hypotonic, but the differences were not statistically significant, possibly because the rates of uptake were too rapid to measure precisely (data not shown). Data presented in Supplemental material demonstrate that  $\text{Ba}^{2+}$  uptake was also stimulated by hypotonic conditions and inhibited by hypertonicity.

The trace labelled CHO in Fig. 8A shows the results of an identical experiment carried out with non-transfected CHO T cells. Practically no  $\text{Ca}^{2+}$  uptake was observed with these cells and there was no effect of changing the osmolarity. The trace shown represents the combined average of duplicate determinations carried out under isotonic, hypotonic and hypertonic conditions.

In Fig. 8B, the procedure was altered in that either isotonic, hypotonic or hypertonic medium (without  $\text{Ca}^{2+}$ ) was applied 2 min prior to beginning the recordings. This allowed cell volume changes to be completed before initiating NCX activity.  $\text{Ca}^{2+}$  (0.1 mM) was then applied in the same isotonic, hypotonic or hypertonic medium, as indicated. Importantly, in this experiment we minimized the duration of solution flow by using the rapid replacement procedure, i.e. the equilibration solution was

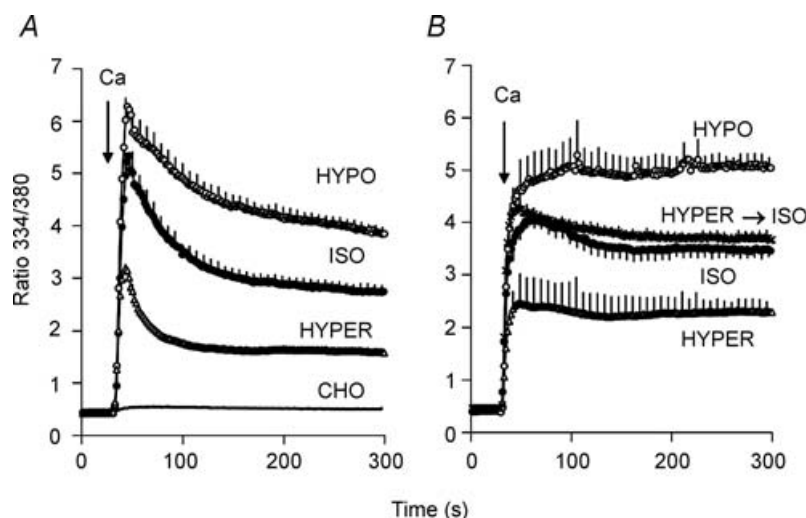


**Figure 8. Effect of osmolarity on  $\text{Ca}^{2+}$  uptake**

A, gramicidin-treated cells expressing  $\Delta(241\text{--}680)$  were equilibrated with 70/70 Na/K-PSS. Two minutes prior to beginning recording, the medium was changed to 70/140 Na/mannitol-PSS.  $\text{Ca}^{2+}$  uptake was initiated by superfusing 5 ml of 0.1 mM  $\text{Ca}^{2+}$  in 70/140 Na/mannitol-PSS (ISO), 70 Na-PSS (HYPO) or 70/500 Na/mannitol-PSS (HYPER). ( $n=4$  for each condition). For the trace labelled CHO, identical experiments were carried out with non-transfected CHO cells. The trace for the non-transfected cells represents the average of duplicate measurements under the isotonic, hypotonic and hypertonic conditions (i.e.  $n=6$ ). B, gramicidin-treated cells were equilibrated in 70/70 Na/K-PSS as described above. Two minutes prior to beginning recordings, the medium was changed to either 70/140 Na/mannitol-PSS (ISO,  $n=4$ ), 70 Na-PSS (HYPO;  $n=3$ ) or 70/500 Na/mannitol-PSS (HYPER,  $n=4$ ). NCX activity was initiated by superfusing 5 ml of 0.1 mM  $\text{Ca}^{2+}$  in the same media, i.e. 70/140 Na/mannitol-PSS (ISO), 70 Na-PSS (HYPO) or 70/500 Na/mannitol-PSS (HYPER). The hypertonic and hypotonic points were significantly different from the isotonic points ( $P < 0.05$ ) at all times after 60 s. For the trace labelled HYPER→ISO, the cells were placed in 70/500 Na/mannitol-PSS 2 min prior to beginning recording, and  $\text{Ca}^{2+}$  uptake was assayed in 70/140 Na/mannitol-PSS ( $n=3$ ).

aspirated and rapidly replaced with the assay medium. The results lead to three important conclusions. First, the effects of osmolarity changes on NCX activity are stable and persist after the changes in cell volume have been completed. Second, the effects of osmolarity are completely and rapidly reversible. For the trace labelled 'Hyper→Iso', the cells were transferred to the hypertonic medium 2 min prior to beginning the recordings but  $\text{Ca}^{2+}$  uptake was then initiated in the isotonic medium. The rate of  $\text{Ca}^{2+}$  uptake was essentially identical to the control (Iso) trace in which cells were in isotonic media throughout the experiment. Third, the peak values for the fura-2 ratio are lower in each case than for the data in panel A, and the post-peak declines in the ratio are markedly attenuated. This suggests that the peak-and-decline behaviour of the  $\text{Ca}^{2+}$  uptake traces illustrated at the outset of this report (Fig. 1) reflects the stimulatory effects of solution flow on NCX activity during superfusion. Thus,  $[\text{Ca}^{2+}]_i$  rapidly rises to a peak value during the application of the assay medium by the superfusion procedure, while the subsequent decline in  $[\text{Ca}^{2+}]_i$  reflects in part the reduction in NCX activity following the cessation of flow.

A comparison of Fig. 8A and B also reveals that the final ratio values at 300 s for the rapid replacement procedure (panel B) were 26, 30 and 44% higher for the isotonic, hypotonic and hypertonic traces (respectively) than for the superfusion procedure (panel A). The significance of this observation is unclear. It might indicate that solution flow, in addition to stimulating NCX activity, also induces a subsequent inactivation of activity once flow ceases. Alternatively, solution flow might stimulate other mechanisms of clearing cytosolic  $\text{Ca}^{2+}$ , such as plasma membrane  $\text{Ca}^{2+}$  ATPase activity or mitochondrial  $\text{Ca}^{2+}$  sequestration. At present, we cannot distinguish between these alternatives.

### Mechanosensitive NCX activity in cardiac myocytes

The data in Fig. 9 address the issue of whether NCX activity is mechanosensitive in cardiac myocytes as well as in transfected CHO cells. In the myocytes,  $\text{Ca}^{2+}$  channel activity interferes with the measurement of NCX activity using either  $\text{Ca}^{2+}$  or  $\text{Ba}^{2+}$  and so we measured  $\text{La}^{3+}$  uptake instead;  $\text{La}^{3+}$  is not conducted by the  $\text{Ca}^{2+}$  channels in neonatal myocytes, but is transported by the  $\text{Na}^+-\text{Ca}^{2+}$  exchanger (Reeves & Condrescu, 2003). Since  $\text{La}^{3+}$  binds with high affinity to the exchanger, a low concentration was used ( $20 \mu\text{M}$ ) to avoid saturating the  $\text{Ca}^{2+}$  translocation sites. As a control, we first measured  $\text{La}^{3+}$  uptake in CHO cells expressing the wild-type NCX (Fig. 9A). Here cells were treated with ATP + Tg as usual and equilibrated with gramicidin in 100/40 Na/K-PSS containing  $30 \mu\text{M}$  EGTA. Trace *a* in Fig. 9A shows  $\text{La}^{3+}$  uptake when initiated by superfusing 15 ml of  $20 \mu\text{M}$   $\text{La}^{3+}$  in 100/40 Na/K-PSS over a 50–60 s period.  $\text{La}^{3+}$  uptake was initially rapid but stopped when fluid flow stopped, as shown by the break in the uptake curve (asterisk in panel A). When initiated by the rapid replacement procedure (trace *b*),  $\text{La}^{3+}$  uptake was less than in trace *a* ( $P < 0.05$  at time points between 45 and 84 s;  $n = 3$ ). The maximal rates of  $\text{La}^{3+}$  uptake were  $4.9 \pm 0.25 \times 10^{-2}$  ratio units  $\text{s}^{-1}$  for the superfusion procedure, and  $2.5 \pm 0.21 \times 10^{-2}$  ratio units  $\text{s}^{-1}$  for the rapid replacement procedure ( $P < 0.002$ ). Thus,  $\text{La}^{3+}$  uptake was stimulated by fluid flow, but the effect was less pronounced than seen in the experiments with  $\text{Ba}^{2+}$  (cf. Fig. 2).

Figure 9B shows an identical experiment carried out with neonatal rat myocytes. Intracellular  $\text{Ca}^{2+}$  stores in the myocytes were depleted with 10 mM caffeine plus  $2 \mu\text{M}$  thapsigargin, but the procedure was otherwise identical to that described for panel A. The results were similar to those obtained with the CHO cells. The rate

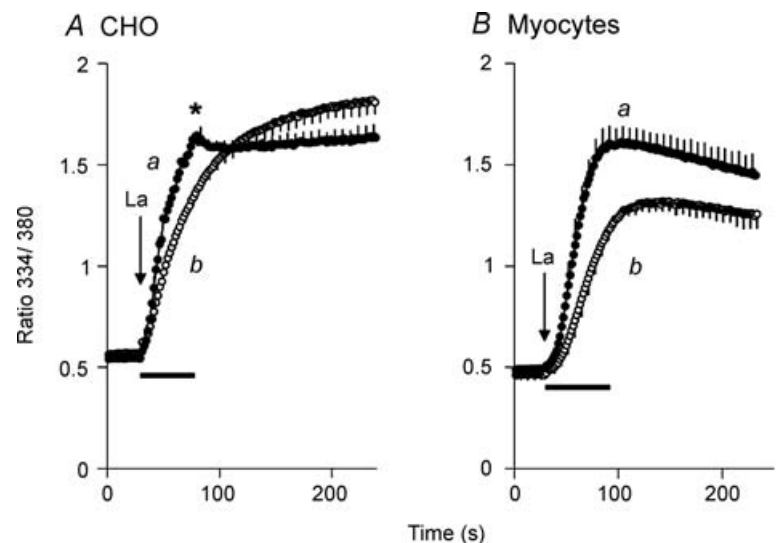


**Figure 9.  $\text{La}^{3+}$  uptake in transfected CHO cells and rat neonatal cardiac myocytes**

A, CHO cells expressing NCX1.1 were treated with ATP + Tg 10 min before beginning recording. At 8 min before recording, cells were treated with gramicidin in 100/40 Na/K-PSS containing  $30 \mu\text{M}$  EGTA. NCX activity was initiated by superfusing 15 ml of  $20 \mu\text{M}$   $\text{LaCl}_3$  in 100/40 Na/K-PSS (trace *a*) over a 50–60 s interval, or by rapidly removing the pre-incubation medium and replacing it with 1 ml of  $20 \mu\text{M}$   $\text{LaCl}_3$  in 100/40 Na/K-PSS (trace *b*). ( $n = 3$ ). B, neonatal rat myocytes were treated with 10 mM caffeine plus  $2 \mu\text{M}$  Tg 10 min prior to beginning recordings. Subsequently, the cells were treated exactly as described for panel A ( $n = 5$ ). The bars below the traces in panels A and B denote the duration of solution superfusion.

of  $\text{La}^{3+}$  uptake initiated by rapid replacement was less than with the superfusion procedure; the data points for the two traces were significantly different between 60 s and 160 s ( $P < 0.05$ ). The maximal rates of  $\text{La}^{3+}$  uptake were  $4.3 \pm 0.43 \times 10^{-2}$  ratio units  $\text{s}^{-1}$  for the superfusion procedure and  $2.1 \pm 0.18 \times 10^{-2}$  ratio units  $\text{s}^{-1}$  for the rapid replacement procedure ( $P < 0.002$ ,  $n = 5$ ). Thus, the rate of  $\text{La}^{3+}$  uptake was approximately 2-fold higher for both rat neonatal myocytes and transfected CHO cells during continuous superfusion of the assay medium.

There were some minor differences between the results with myocytes and CHO cells. Thus,  $\text{La}^{3+}$  uptake in myocytes did not display the abrupt change in rate shown by the CHO cells when superfusion ceased (asterisk in Fig. 9A). Also, unlike the CHO cells, the myocytes displayed short delays before maximal rates of  $\text{La}^{3+}$  uptake were observed. The reasons for these differences are not clear at present.

## Discussion

Several years ago we adopted a simple procedure for initiating NCX activity while monitoring fura-2 fluorescence by digital imaging, i.e. manually superfusing the cells with 4–5 ml of the assay solution while maintaining constant aspiration. In this report, we demonstrate that NCX activity was stimulated during the resulting solution flow and declined following the cessation of flow. In the case of  $\text{Ba}^{2+}$ , this leads to a sharply biphasic time course of uptake in which the rate of uptake during the initial rapid phase is more than 10 times greater than during the subsequent slow phase (Fig. 2). During  $\text{Ca}^{2+}$  uptake,  $[\text{Ca}^{2+}]_i$  rises to a peak and then declines to a lower steady-state value. The situation is highly complex in the case of  $\text{Ca}^{2+}$ , since there are multiple mechanisms that affect the cytosolic  $\text{Ca}^{2+}$  concentration. Thus, mitochondrial  $\text{Ca}^{2+}$  accumulation and  $\text{Ca}^{2+}$  efflux by the plasma membrane  $\text{Ca}^{2+}$  ATPase both contribute to reducing  $[\text{Ca}^{2+}]_i$  following the peak attained after the initiation of reverse mode NCX (Fig. 1). Nevertheless, these processes would not be expected to produce the large post-peak declines that we observe unless there was also a diminution in the rate of  $\text{Ca}^{2+}$  influx.

When we used an alternative procedure for changing solutions, i.e. removing the pre-incubation medium and quickly replacing it with the assay medium, the initial stimulation of exchange activity was greatly reduced, as shown by the much smaller magnitude of the rapid phase of  $\text{Ba}^{2+}$  uptake (Figs 2 and 3). When  $\text{Ca}^{2+}$  uptake was initiated using the rapid replacement procedure, both the peak fura ratio and the subsequent decline were attenuated (Fig. 8B). With the rapid replacement procedure, the duration of the solution flow was limited to 2–3 s, as opposed to the ~20 s normally used for the superfusion procedure. Extending the duration of superfusion for a period of 80 s stimulated exchange activity for the entire time the

solution was applied (Fig. 3). Multiple periods of superfusion stimulated exchange activity multiple times (Fig. 4), although there were no changes in ionic composition after the first solution application. Finally, the superfusion procedure stimulated both the reverse and forward modes of NCX activity (Fig. 5), as well as the  $\text{Ca}^{2+}$ – $\text{Ba}^{2+}$  exchange mode (Fig. 6). We conclude that the mechanical effects of solution flow stimulate NCX activity. Since  $\text{Ca}^{2+}$ – $\text{Ba}^{2+}$  exchange is stimulated in the absence of  $\text{Na}^+$ , these effects cannot be attributed to possible alterations in the cytosolic  $\text{Na}^+$  concentration.

During superfusion, the fluorescence intensities of fura-2 at both excitation wavelengths declined, then partially recovered following cessation of flow (Fig. 7). This probably reflects small displacements of the cell relative to the area of interest monitored during fluorescence measurements and/or a partial loss of focus during flow. It is conceivable that these intensity alterations could induce an artifactual rise in the apparent rate of  $\text{Ca}^{2+}$  or  $\text{Ba}^{2+}$  influx during superfusion. This is clearly not the case, however, since any such artifacts should also be apparent in assays of  $\text{Ba}^{2+}$  influx via store-operated channels, whereas, in fact, this mode of  $\text{Ba}^{2+}$  entry was only slightly stimulated by superfusion (Fig. 2C).

The mechanism underlying flow-dependent stimulation of activity is unclear. Cytoskeletal interactions are probably not involved since the  $\Delta(241\text{--}680)$  mutant used for most of these studies does not interact with the cytoskeleton (Condrescu & Reeves, 2006). Moreover, agents affecting the cytoskeleton (cytochalasin D, nocodazole, plating cells on polylysine) had no obvious effect on the results (data not shown). A broad spectrum protein kinase inhibitor, staurosporine, did not alter the biphasic nature of  $\text{Ba}^{2+}$  uptake, suggesting that changes in protein phosphorylation are not involved (data not shown).

Mechanosensitivity of channel-forming ionophores and natural ion channels may reflect a hydrophobic mismatch between the lipid bilayer and hydrophobic transmembrane regions, so that channel conformations are altered by changes in membrane tension (Hamill & Martinac, 2001; Hwang *et al.* 2003). It seems possible that the conformational changes associated with carrier-mediated ion translocation might be subject to similar constraints. Although agents likely to influence hydrophobic mismatch, i.e.  $\beta$ -octylglucoside (5 mM) and cholesterol extraction with 10 mM  $\beta$ -Me-cyclodextrin (Lundbaek *et al.* 2004), did not alter the biphasic nature of NCX-mediated  $\text{Ba}^{2+}$  uptake (data not shown), this possibility deserves further exploration.

A second possible mechanism could be a flow-dependent unfolding of the plasma membrane, exposing exchangers sequestered within membrane invaginations or submembrane vesicles. We tested this possibility using a haemagglutinin (HA) epitope-tagged exchanger,

following the procedures previously described (Condrescu & Reeves, 2006), but were unable to detect a change in surface expression with flow (data not shown). However, the additional membrane exposure might be transient and/or not revealed by the cell fixation procedures involved in this assay. A related possibility is that mechanical perturbations might disrupt a diffusion barrier between the submembrane space and the bulk cytosol, thereby promoting net  $\text{Ca}^{2+}$  or  $\text{Ba}^{2+}$  entry to the cytosol. Since  $\text{Ba}^{2+}$  influx through store-operated channels was much less affected by superfusion than NCX activity (Fig. 2C), this possibility seems unlikely, unless one also postulates selective compartmentation of NCX.

Osmotically induced changes in cell volume also altered NCX activity. In our experiments, hypotonicity stimulated, and hypertonicity inhibited NCX activity. Our results differ from those reported by Wright *et al.* (1995), who observed that hypotonicity produced a time-dependent decline in NCX currents in guinea pig ventricular myocytes, whereas hypertonicity produced a transient increase in current followed by a gradual decline. At present, we have no explanation for the difference between their results and ours. However, hypertonicity has been reported to induce a time-dependent (minutes) increase in cellular  $\text{PIP}_2$  levels in cardiac myocytes and HeLa cells (Nasuhoglu *et al.* 2002; Yamamoto *et al.* 2006), and this might simulate NCX activity under certain conditions. In the experiments of Wright *et al.* (1995) the inhibitory effects of hypotonicity developed over a period of several minutes, consistent with a time-dependent change in  $\text{PIP}_2$ . In our experiments, the effects of osmotic changes on NCX activity occur over a much faster time course (seconds), the same time range in which osmotic volume changes occur, consistent with a direct mechanical effect on the exchanger.

The changes in NCX activity with flow are more striking for  $\text{Ba}^{2+}$  uptake than for  $\text{Ca}^{2+}$  uptake. Thus, there is a dramatic difference between the effects of the superfusion and rapid replacement procedures on  $\text{Ba}^{2+}$  uptake (Fig. 2), but the difference is less pronounced in the case of  $\text{Ca}^{2+}$  uptake (compare Fig. 8A and B). Moreover, NCX-mediated  $\text{Ba}^{2+}$  efflux is relatively modest in the absence of solution flow (Fig. 5B). In contrast,  $\text{Na}^+$ -dependent  $\text{Ca}^{2+}$  efflux occurs rapidly under static conditions, as shown by the ability of NCX activity to sharply attenuate  $\text{Ca}^{2+}$  transients induced by the addition of ionomycin, ATP or Tg under conditions involving minimal solution flow (e.g. Chernysh *et al.* 2004). This behaviour may reflect special constraints on  $\text{Ba}^{2+}$  transport because of its larger ionic radius (0.134 nm) compared to  $\text{Ca}^{2+}$  (0.099 nm).  $\text{Ba}^{2+}$  uptake is also more sensitive to temperature (Trac *et al.* 1997) and reduced pH (data not shown) than  $\text{Ca}^{2+}$  uptake.  $\text{La}^{3+}$  uptake also appeared to be less sensitive to the effects of fluid flow than  $\text{Ba}^{2+}$  uptake. With  $\text{La}^{3+}$  (ionic radius 0.102 nm), a 2-fold

stimulation of uptake was observed during superfusion compared to the rapid replacement procedure (Fig. 9).

Importantly, the use of  $\text{La}^{3+}$  allowed us to demonstrate that mechanosensitivity of NCX activity is not simply a peculiarity of heterologous expression in transfected CHO cells, but was also displayed by the native NCX in neonatal rat cardiac myocytes (Fig. 9B). Thus, as in CHO cells, the maximal rates of  $\text{La}^{3+}$  uptake were stimulated 2-fold when exchange activity was initiated by superfusion compared to the rapid replacement procedure. Given the similar behaviour of the CHO cells and cardiac myocytes, we speculate that the mechanism underlying NCX mechanosensitivity may be intrinsic to NCX itself, rather than an effect of membrane trafficking, for example, or other secondary influences that would be likely to differ between the two cell types.

The mechanosensitivity of  $\text{Na}^+$ - $\text{Ca}^{2+}$  exchange activity could be physiologically important in several settings. The laminar structure of the myocardium leads to significant shear forces during normal cardiac functioning (Costa *et al.* 1999; Ashikaga *et al.* 2004) that could influence NCX activity. Changes in intramyocardial pressure during the contraction cycle might also serve to modulate exchange activity. Following acute cardiac ischaemia, the stimulation of reverse NCX activity by cell swelling could increase the potential for arrhythmogenic exchange currents and/or  $\text{Ca}^{2+}$  overload. In vascular endothelial cells, flow-dependent changes in NCX activity might play a significant role in modulating endothelial NO production (Schneider *et al.* 2002). These examples suggest that further investigations into the mechanical properties of the  $\text{Na}^+$ - $\text{Ca}^{2+}$  exchanger could lead to novel insights into its role in regulating myocardial and vascular functions.

## References

- Abdellatif M, MacLellan WR & Schneider MD (1994). p21 Ras as a governor of global gene expression. *J Biol Chem* **269**, 15423–15426.
- Alexander RT & Grinstein S (2006).  $\text{Na}^+/\text{H}^+$  exchangers and the regulation of volume. *Acta Physiol (Oxf)* **187**, 159–167.
- Ashikaga H, Criscione JC, Omens JH, Covell JW & Ingels NB Jr (2004). Transmural left ventricular mechanics underlying torsional recoil during relaxation. *Am J Physiol Heart Circ Physiol* **286**, H640–H647.
- Bewick NL, Fernandes C, Pitt AD, Rasmussen HH & Whalley DW (1999). Mechanisms of  $\text{Na}^+$ - $\text{K}^+$  pump regulation in cardiac myocytes during hyposmolar swelling. *Am J Physiol Cell Physiol* **276**, C1091–C1099.
- Chernysh O, Condrescu M & Reeves JP (2004). Calcium-dependent regulation of calcium efflux by the cardiac sodium/calcium exchanger. *Am J Physiol Cell Physiol* **287**, C797–C806.
- Condrescu M, Chernaya G, Kalaria V & Reeves JP (1997). Barium influx mediated by the cardiac sodium-calcium exchanger in transfected Chinese hamster ovary cells. *J Gen Physiol* **109**, 41–51.

- Condrescu M & Reeves JP (2006). Actin-dependent regulation of the cardiac  $\text{Na}^+/\text{Ca}^{2+}$  exchanger. *Am J Physiol Cell Physiol* **290**, C691–C701.
- Costa KD, Takayama Y, McCulloch AD & Covell JW (1999). Laminar fiber architecture and three-dimensional systolic mechanics in canine ventricular myocardium. *Am J Physiol Heart Circ Physiol* **276**, H595–H607.
- Dong H, Dunn J & Lytton J (2002). Stoichiometry of the cardiac  $\text{Na}^+/\text{Ca}^{2+}$  exchanger NCX1.1 measured in transfected HEK cells. *Biophys J* **82**, 1943–1952.
- Fujioka Y, Komeda M & Matsuoka S (2000). Stoichiometry of  $\text{Na}^+-\text{Ca}^{2+}$  exchange in inside-out patches excised from guinea-pig ventricular myocytes. *J Physiol* **523**, 339–351.
- Fuster D, Moe OW & Hilgemann DW (2004). Lipid- and mechanosensitivities of sodium/hydrogen exchangers analyzed by electrical methods. *Proc Natl Acad Sci U S A* **101**, 10482–10487.
- Gautam M, Gojova A & Barakat AI (2006). Flow-activated ion channels in vascular endothelium. *Cell Biochem Biophys* **46**, 277–284.
- Gu CX, Juranka PF & Morris CE (2001). Stretch-activation and stretch-inactivation of Shaker-IR, a voltage-gated  $\text{K}^+$  channel. *Biophys J* **80**, 2678–2693.
- Haas M & Forbush B III (1998). The Na-K-Cl cotransporters. *J Bioenerg Biomembr* **30**, 161–172.
- Hamill OP & Martinac B (2001). Molecular basis of mechanotransduction in living cells. *Physiol Rev* **81**, 685–740.
- Hwang TC, Koeppe RE & Andersen OS (2003). Genistein can modulate channel function by a phosphorylation-independent mechanism: importance of hydrophobic mismatch and bilayer mechanics. *Biochemistry* **42**, 13646–13658.
- Kang TM & Hilgemann DW (2004). Multiple transport modes of the cardiac  $\text{Na}^+/\text{Ca}^{2+}$  exchanger. *Nature* **427**, 544–548.
- Kong CR, Bursac N & Tung L (2005). Mechanoelectrical excitation by fluid jets in monolayers of cultured cardiac myocytes. *J Appl Physiol* **98**, 2328–2336.
- Lambert IH (2004). Regulation of the cellular content of the organic osmolyte taurine in mammalian cells. *Neurochem Res* **29**, 27–63.
- Langille SE, Patki V, Klarlund JK, Buxton JM, Holik JJ, Chawla A, Corvera S & Czech MP (1999). ADP-ribosylation factor 6 as a target of guanine nucleotide exchange factor GRP1. *J Biol Chem* **274**, 27099–27104.
- Lorenzen-Schmidt I, Schmid-Schonbein GW, Giles WR, McCulloch AD, Chien S & Omens JH (2006). Chronotropic response of cultured neonatal rat ventricular myocytes to short-term fluid shear. *Cell Biochem Biophys* **46**, 113–122.
- Lundbaek JA, Birn P, Hansen AJ, Sogaard R, Nielsen C, Girshman J, Bruno MJ, Tape SE, Egebjerg J, Greathouse DV, Mattice GL, Koeppe RE & Andersen OS (2004). Regulation of sodium channel function by bilayer elasticity: the importance of hydrophobic coupling. Effects of Micelle-forming amphiphiles and cholesterol. *J Gen Physiol* **123**, 599–621.
- Lytton J, Westlin M & Hanley MR (1991). Thapsigargin inhibits the sarcoplasmic or endoplasmic reticulum Ca-ATPase family of calcium pumps. *J Biol Chem* **266**, 17067–17071.
- Matsuoka S, Nicoll DA, Reilly RF, Hilgemann DW & Philipson KD (1993). Initial localization of regulatory regions of the cardiac sarcolemmal  $\text{Na}^+-\text{Ca}^{2+}$  exchanger. *Proc Natl Acad Sci U S A* **90**, 3870–3874.
- Muallem S, Zhang BX, Loessberg PA & Star RA (1992). Simultaneous recording of cell volume changes and intracellular pH or  $\text{Ca}^{2+}$  concentration in single osteosarcoma cells UMR-106-01. *J Biol Chem* **267**, 17658–17664.
- Nasuhoglu C, Feng S, Mao Y, Shammatt I, Yamamoto M, Earnest S, Lemmon M & Hilgemann DW (2002). Modulation of cardiac PIP2 by cardioactive hormones and other physiologically relevant interventions. *Am J Physiol Cell Physiol* **283**, C223–C234.
- Numata T, Shimizu T & Okada Y (2007). Direct mechano-stress sensitivity of TRPM7 channel. *Cell Physiol Biochem* **19**, 1–8.
- Oancea E, Wolfe JT & Clapham DE (2006). Functional TRPM7 channels accumulate at the plasma membrane in response to fluid flow. *Circ Res* **98**, 245–253.
- Opuni K & Reeves JP (2000). Feedback inhibition of sodium/calcium exchange by mitochondrial calcium accumulation. *J Biol Chem* **275**, 21549–21554.
- Park SW, Byun D, Bae YM, Choi BH, Park SH, Kim B & Cho SI (2007). Effects of fluid flow on voltage-dependent calcium channels in rat vascular myocytes: fluid flow as a shear stress and a source of artifacts during patch-clamp studies. *Biochem Biophys Res Commun* **358**, 1021–1027.
- Pedersen SF, O'Donnell ME, Anderson SE & Cala PM (2006). Physiology and pathophysiology of  $\text{Na}^+/\text{H}^+$  exchange and  $\text{Na}^+-\text{K}^+-2\text{Cl}^-$  cotransport in the heart, brain, and blood. *Am J Physiol Regul Integr Comp Physiol* **291**, R1–R25.
- Peng SQ, Hajela RK & Atchison WD (2005). Fluid flow-induced increase in inward  $\text{Ba}^{2+}$  current expressed in HEK293 cells transiently transfected with human neuronal L-type  $\text{Ca}^{2+}$  channels. *Brain Res* **1045**, 116–123.
- Perozo E, Kloda A, Cortes DM & Martinac B (2002). Physical principles underlying the transduction of bilayer deformation forces during mechanosensitive channel gating. *Nat Struct Biol* **9**, 696–703.
- Reeves JP & Condrescu M (2003). Lanthanum is transported by the sodium/calcium exchanger and regulates its activity. *Am J Physiol Cell Physiol* **285**, C763–C770.
- Reeves JP & Hale CC (1984). The stoichiometry of the cardiac sodium-calcium exchange system. *J Biol Chem* **259**, 7733–7739.
- Satlin LM, Carattino MD, Liu W & Kleyman TR (2006). Regulation of cation transport in the distal nephron by mechanical forces. *Am J Physiol Renal Physiol* **291**, F923–F931.
- Schneider JC, El Kebir D, Chereau C, Mercier JC, Dall'Ava-Santucci J & Dihl-Xuan AT (2002). Involvement of  $\text{Na}^+/\text{Ca}^{2+}$  exchanger in endothelial NO production and endothelium-dependent relaxation. *Am J Physiol Heart Circ Physiol* **283**, H837–H844.
- Trac M, Dyck C, Hnatowich M, Omelchenko A & Hryshko IV (1997). Transport and regulation of the cardiac  $\text{Na}^+-\text{Ca}^{2+}$  exchanger, NCX1. Comparison between  $\text{Ca}^{2+}$  and  $\text{Ba}^{2+}$ . *J Gen Physiol* **109**, 361–369.

- Urbanczyk J, Chernysh O, Condrescu M & Reeves JP (2006). Sodium-calcium exchange does not require allosteric calcium activation at high cytosolic sodium concentrations. *J Physiol* **575**, 693–705.
- Venosa RA (1991). Hypo-osmotic stimulation of active Na<sup>+</sup> transport in frog muscle: apparent upregulation of Na<sup>+</sup> pumps. *J Membr Biol* **120**, 97–104.
- Venosa RA (2003). Hypotonic stimulation of the Na<sup>+</sup> active transport in frog skeletal muscle: role of the cytoskeleton. *J Physiol* **548**, 451–459.
- Whalley DW, Hool LC, Ten Eick RE & Rasmussen HH (1993). Effect of osmotic swelling and shrinkage on Na<sup>+</sup>-K<sup>+</sup> pump activity in mammalian cardiac myocytes. *Am J Physiol Cell Physiol* **265**, C1201–C1210.
- Wright AR, Rees SA, Vandenberg JI, Twist VW & Powell T (1995). Extracellular osmotic pressure modulates sodium-calcium exchange in isolated guinea-pig ventricular myocytes. *J Physiol* **488**, 293–301.
- Yamamoto M, Chen MZ, Wang YJ, Sun HQ, Wei Y, Martinez M & Yin HL (2006). Hypertonic stress increases phosphatidylinositol 4,5-bisphosphate levels by activating PIP5K1b. *J Biol Chem* **281**, 32630–32638.

## Acknowledgements

We thank Dr Roman Shirokov for the use of his osmometer and for his comments on the manuscript. Thanks also to Olga Chernysh for assistance in obtaining the images of calcein-loaded cells shown in Supplemental material. This work was supported by NIH grant HL-49932.

## Supplemental material

Online supplemental material for this paper can be accessed at: <http://jp.physoc.org/cgi/content/full/jphysiol.2008.151274/DC1> and <http://www.blackwell-synergy.com/doi/suppl/10.1113/jphysiol.2008.151274>